Environmental and Climate Technologies
2025, vol. 29, no. 1, pp. 940–959
https://doi.org/10.2478/rtuect-2025-0063
https://content.sciendo.com

1862
RIGA TECHNICAL UNIVERSITY

Comparative Analysis of Cement-Asbestos Materials from Poland and Lithuania: Thermal Decomposition, Mineralogical Characterisation, and Implications for Recycling

Robert KUSIOROWSKI[1*], Anna GERLE[2], Magdalena KUJAWA[3], Valentin ANTONOVIČ[4], Renata BORIS[5]

[1–3]*Łukasiewicz Research Network – Institute of Ceramics and Building Materials, Cementowa 8, 31-983 Cracow; Center of Refractory Materials, Toszecka 99, 44-100 Gliwice, Poland*

[4,5]*Laboratory of Composite Materials, Institute of Building Materials, Faculty of Civil Engineering, Vilnius Gediminas Technical University, Linkmenu St. 28, 08217 Vilnius, Lithuania*

Received 17.04.2025; accepted 26.11.2025

***Abstract* – Asbestos-containing cement materials were widely used in construction in the past due to their durability, fire resistance, and thermal insulation properties. However, asbestos is now recognised as a carcinogenic material and has been banned in many countries, including Poland and Lithuania. Asbestos-containing waste is hazardous and requires safe disposal, posing significant environmental challenges. Thermal treatment has been proposed as a potential method for neutralising asbestos and material recycling. In this study, four cement-asbestos samples from Poland (P1, P2) and Lithuania (L1, L2) were investigated to evaluate their chemical composition, mineralogical phases, and thermal behaviour. Samples were characterised using X-ray fluorescence (XRF), X-ray powder diffraction (XRD), differential thermal analysis (DTA), thermogravimetric analysis (TG/DTG), scanning electron microscopy (SEM), and high-temperature microscopy (HTM). Computer simulations of liquid phase formation were performed using FactSage software. The results revealed significant differences between samples from the two countries. Lithuanian materials exhibited higher SiO_2 content and formed liquid phases at lower temperatures, while Polish samples, richer in CaO, showed higher thermal stability and distinct phase evolution. These differences are attributed to variations in raw materials and production methods. The study demonstrates that thermal treatment can effectively transform cement-asbestos materials, with the resulting mineral phases and liquid formation influenced by the initial chemical composition. The findings provide valuable guidance for potential recycling strategies of neutralised asbestos waste, offering an environmentally safer approach to asbestos management.**

***Keywords* – Asbestos waste; cement-asbestos materials; FactSage calculation; mineralogical composition; thermal treatment.**

1. INTRODUCTION

Asbestos is a name for a group of naturally occurring fibrous minerals that have been widely used in industry for many years, especially in construction, due to their insulating, fire-

* Corresponding author.
E-mail address: robert.kusiorowski@icimb.lukasiewicz.gov.pl

resistant, and mechanical strength properties [1]. Its popularity was due to its low price and availability, as well as its ability to withstand high temperatures and aggressive chemicals [2]. The most popular in the past was so-called white asbestos. From the mineralogical point of view, this is chrysotile, hydrated magnesium silicate with the ideal chemical formula $Mg_3Si_2O_5(OH)_4$. Unfortunately, despite its advantages, asbestos poses a significant and well-documented threat to human health. Inhalation of fine, respirable asbestos fibres can lead to severe and often progressive lung diseases, including chronic asbestosis, malignant lung cancer, and aggressive pleural mesothelioma [3], [4], primarily used which led to the gradual withdrawal of this material from use around the world. Today, asbestos is a banned substance in many countries, including European Union member states, the United States, Canada, Australia, and Japan, due to its carcinogenic properties and the severe health risks associated with inhalation of asbestos fibres. Consequently, its removal and disposal have become key challenges in industrial waste management and public health protection [5]–[11].

The Baltic and Central and Eastern European countries, especially post-Soviet could be indicated as an example of countries where asbestos was used on a large scale in the past. For example, in Poland and Lithuania, asbestos was widely used in construction and the chemical and energy industries in the second half of the 20th century. Poland was one of the largest producers of asbestos-containing products in Europe, and asbestos was used in roofing, pipes, insulation, and construction materials, mainly in the form of cement-asbestos products. In both countries, despite the bans on the production and use of asbestos, there is still a problem with removing asbestos materials from existing buildings and other facilities. Data shows that there are still about 15 million tons of asbestos-containing products in Poland and c.a. 4 million tons in Lithuania, only some of which have already been removed [12]–[14]. Many buildings still have asbestos roofing, pipes, or insulation, which degrade over time, releasing dangerous fibres into the air. The lack of appropriate funds for the comprehensive removal of asbestos from private properties remains a problem, as not all owners can bear the costs associated with its safe removal. Although there are government and local programs that offer subsidies for asbestos removal, the pace of work is still too slow compared to the scale of the problem.

One of the promising methods for addressing the problem of asbestos-containing waste, in addition to its disposal through landfilling, is thermal treatment, which has been increasingly investigated in recent years [15]–[17]. Asbestos minerals, belonging to the group of hydrated silicates, undergo dehydroxylation and structural collapse when exposed to elevated temperatures, leading to the formation of new, non-fibrous crystalline phases such as forsterite or enstatite in the case of chrysotile asbestos. Numerous recent studies have shown that this transformation begins around 600–700 °C and becomes complete at temperatures typically exceeding 900–1000 °C, depending on mineral type and heating conditions [18]–[21]. In the case of cement–asbestos materials, the process is more complex due to the presence of a heterogeneous cementitious matrix, which introduces additional thermal reactions, phase transitions, and kinetic constraints [22]–[27]. Thermal-analysis studies on cement–asbestos wastes heated to high temperatures (e.g., 1100 °C) demonstrate that dehydration, dehydroxylation, and recrystallisation into stable phases occur, in some cases via pseudomorphism [28], [29]. Recent research highlights that interactions between chrysotile fibers and the calcium-silicate-hydrate (C–S–H) phases, as well as possible carbonation products, may significantly influence decomposition pathways, reaction rates, and the morphology of the resulting phases [30]. Importantly, several recent works demonstrate that properly optimised thermal treatment not only eliminates the hazardous fibrous structure of asbestos but also yields stable, mineralogically transformed products that can be considered valuable secondary raw materials. For instance, a study on end-of-life fiber

cement boards showed that thermal treatment above 1000 °C fully converts chrysotile into forsterite and enstatite, enabling reuse of the material in sustainable construction applications [31]. Moreover, after thermal calcination, cement mortars modified with treated cement–asbestos waste exhibited favourable mechanical properties, indicating practical potential for recycling [32]. Alternative high-temperature approaches have also been explored: for example, carbothermal reduction of asbestos tailings (with added carbon) yields stable high-temperature composites composed of forsterite and silicon carbide, suggesting another viable pathway for transforming hazardous waste into functional materials [33]. However, most of these studies analysed single types of materials from specific regions, without comparing chemical composition and thermal behaviour across different countries.

The present study addresses this gap by performing a comparative analysis of cement-asbestos materials from Poland and Lithuania, combining chemical, mineralogical, and thermal characterisation with computer simulations of liquid phase formation. This approach allows for a more comprehensive understanding of how material origin and composition influence thermal behaviour and recycling potential, highlighting the practical relevance of the findings for waste management and secondary raw material utilisation.

2. MATERIALS AND METHODS

Four cement–asbestos materials in the form of corrugated roof panels coming from different regions of Lithuania and Poland were tested. There is no detailed information about the conditions of their long-term use. They were named like L1, L2, P1 and P2, respectively. All these materials were tested after crushing and grinding to a grain size below 0.1 mm.

These cement–asbestos samples were comparatively studied using several complementary techniques: X-ray fluorescence (XRF) for chemical composition analysis, differential thermal analysis (DTA) and thermogravimetric analysis (TG/DTG) to study thermal decomposition and mass changes, X-ray powder diffraction (XRD) for phase identification, scanning electron microscopy (SEM) for microstructural characterization, and high-temperature microscopy (HTM) to observe the behaviour of materials at elevated temperatures. Moreover, engineering software FactSage was used to simulate the melting point and the amount of liquid phase during thermal treatment. In addition, all cement–asbestos samples were isothermally calcined at 1100 °C for 2 h in a laboratory furnace (model LT 9/14, Nabertherm, Lilienthal, Germany), and phase analysis was checked (XRD). This temperature was chosen based on the literature [27].

Differential thermal analysis (DTA) and thermogravimetric analysis (TG/DTG) were performed using an STA 409 PC Luxx thermal analyser (Netzsch, Selb, Germany). All experiments were performed at up to 1000 °C in an airflow of 30 mL min^{-1} at a heating rate of 20 K min^{-1} using an open alumina crucible with about 100 mg of sample. For the phase analysis of the cement–asbestos samples, X-ray powder diffraction (PANalytical X'pert Pro diffractometer, CuKα radiation, Ni filter, 40 kV, 30 mA, X'Celerator detector, Malvern PANalytical, Almelo, The Netherlands) was used. The phase composition was determined through the diffraction peaks connecting with the identified phases using HighScore Plus software (version 5.2; Malvern PANalytical, Almelo, The Netherlands) and the ICDD PDF-5+ database. The chemical composition analysis using X-ray fluorescence (XRF) was performed by EN ISO 12677:2011. The samples were measured using the PANalytical MagiX PW2424 spectrometer (Malvern PANalytical, Almelo, The Netherlands). Microstructure analysis was performed using a Mira 3 electron microscope (Tescan, Brno, Czech Republic) equipped with an energy-dispersive spectrometer (EDS) system with AZtec Automated ver. 3.1 software (Oxford Instruments, Abingdon, UK). The measurements were carried out on

the samples covered by a conductive layer of chromium by using a Quorum Q150R ES device (Quorum Technologies, Laughton, UK). The high-temperature microscopic measurements were performed in a high-temperature microscope (Leitz). Cube-shaped samples (edge dimension of 3 mm) of ground material were prepared for tests. The measurement was carried out in an air atmosphere at a constant heating rate of 5 K min^{-1} up to the temperature of 1500 °C. The computer simulations in FactSage software (version 6.4; Thermfact/CRCT, Montreal, Canada, and GTT-Technologies, Aachen, Germany) were used in this study. The module "Equilib" with the "FactPS" and "FToxid" databases was selected for this evaluation. Based on the chemical composition of the tested cement-asbestos samples, the calculations were made to determine the amount of the liquid phase that appears in the considered system in equilibrium state, depending on the temperature from the range 900–1300 °C and pressure of 1 atm. The simulation was based on determining the amount of liquid phase produced from 100 g of raw material. The calculations of the liquid phase took into account the full chemical composition, while in the case of the location of points in the CaO-MgO-SiO_2 system, the mutual proportions of the above oxides were taken into account.

3. RESULTS

All tested samples contained characteristic bundles of asbestos fibres, which were clearly visible after fragmentation for research. In each case, the fibres of various lengths and widths were observed. The fibre bundles showed a tendency to split into smaller, elementary fibres (Fig. 1).

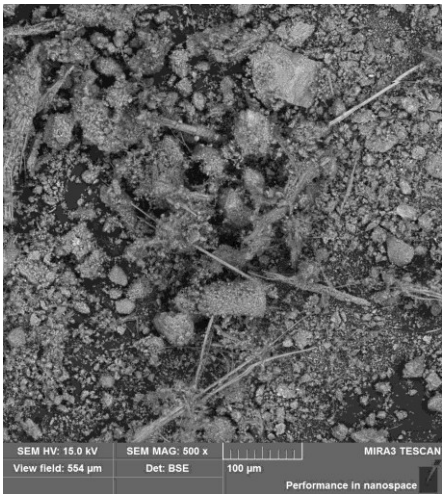

Fig. 1. An example SEM image of crushed cement-asbestos with a bundle of asbestos fibers.

The chemical composition of the tested cement-asbestos shows (Table 1) that it is dominated by SiO_2 and CaO. It is worth noting that for samples from Lithuania, the silicon oxide amount is much higher, while in samples from Poland, the calcium oxide is dominant. The very high loss on ignition value is also noteworthy, which has changed from ~20 to 25 wt%. Besides these components, there are also presented accompanying ingredients like MgO (ca 4–6 wt%), iron compounds (3–5 wt%), and Al_2O_3 (ca 4 wt%). The presence of magnesium oxide in the chemical analysis can be connected directly with the chrysotile

asbestos. MgO is one of the main oxides included in the chemical formula of white asbestos. Cement-asbestos samples from Lithuania have visible a higher amount of MgO, which can indicate a higher content of asbestos fibres in the samples, or is the effect of long-term ageing of materials and gradual leaching of cementitious matrix in the external environment.

Moreover, samples from Poland also have a visibly higher amount of sulphur, which is five times greater than Lithuanian samples. This phenomenon can be explained, probably by the origin of the samples. Polish samples (P1, P2) come from the Upper Silesia region, the most heavily industrialised in Poland, where some specific phenomena occur. In this region, energy production is mainly based on hard coal burning, which results in intensive emission of acidic gases and solid particles, which may contribute to the formation of acid rain enriched with sulphur compounds [34].

TABLE 1. CHEMICAL ANALYSIS OF CEMENT-ASBESTOS SAMPLES

Sample name	**L1**	**L2**	**P1**	**P2**
Country	Lithuania	Lithuania	Poland	Poland
SiO_2	33.1 ± 1.5	33.4 ± 1.5	20.1 ± 0.9	18.6 ± 0.9
Al_2O_3	3.6 ± 0.3	3.8 ± 0.3	4.6 ± 0.3	3.8 ± 0.3
Fe_2O_3	5.2 ± 0.1	3.4 ± 0.1	3.0 ± 0.1	2.5 ± 0.1
MgO	6.5 ± 0.5	5.7 ± 0.4	3.5 ± 0.4	4.5 ± 0.4
CaO	25.5 ± 1.2	33.5 ± 1.6	43.0 ± 2.0	46.0 ± 2.1
Na_2O+K_2O	0.7 ± 0.2	0.4 ± 0.2	0.4 ± 0.2	0.3 ± 0.2
SO_3	0.3 ± 0.1	0.4 ± 0.1	2.2 ± 0.4	1.7 ± 0.3
LOI	24.7 ± 2.5	18.8 ± 1.8	21.8 ± 2.2	22.2 ± 2.2

Fig. 2 presents the comparison of X-ray powder diffraction patterns of all tested raw cement–asbestos samples. Even though the samples were exposed to the action of external conditions in varying degrees and times, the phase compositions for the tested samples were rather similar, especially between individual countries. Tested samples P1 and P2, or L1 and L2, were similar to each other, respectively. On the X-ray diffraction patterns of all samples, diffraction reflexes from the cementitious matrix dominate. The main identified crystal components for all samples were calcium carbonate in the crystal form of calcite ($CaCO_3$; ICDD-PDF 04-012-8072). As an asbestos mineral for all samples, a chrysotile variant ($Mg_3Si_2O_5(OH)_4$; ICDD-PDF 00-027-1276) was identified. This was confirmed by the presence of the characteristic narrow and intense two major diffraction reflexes at d_{002} = 7.32 Å and d_{004} = 3.65 Å of white asbestos visible at ~12° and ~24° 2Theta, respectively [35].

Besides the above-mentioned phases, other mineral phases were also identified. For samples from both countries phases like ettringite ($Ca_6(Al(OH)_6)_2(SO_4)_2 \cdot 26H_2O$; ICDD-PDF 01-073-6239), larnite (Ca_2SiO_4; ICDD-PDF 01-083-0464), hatrurite (Ca_3SiO_5; ICDD-PDF 01-070-8632) were identified. They come directly on a cementitious matrix. X-ray reflexes coming from these phases were clearly visible in the case of Polish samples, which may indicate a relatively low degree of carbonisation and ageing of the samples from Poland in comparison with Lithuanian samples. Moreover, traces of gypsum ($CaSO_4 \cdot 2H_2O$; ICDD-PDF 04-015-4421) as well as katoite ($Ca_3Al_2(SiO_4)_{0.7}(OH)_{9.3}$; ICDD-PDF 04-026-3599) were also stated. In relation to gypsum, the X-ray intensity of reflexes was higher for the Polish materials, especially for the P1 sample, which may prove the validity of the phenomenon related to the increased content of sulphate compounds.

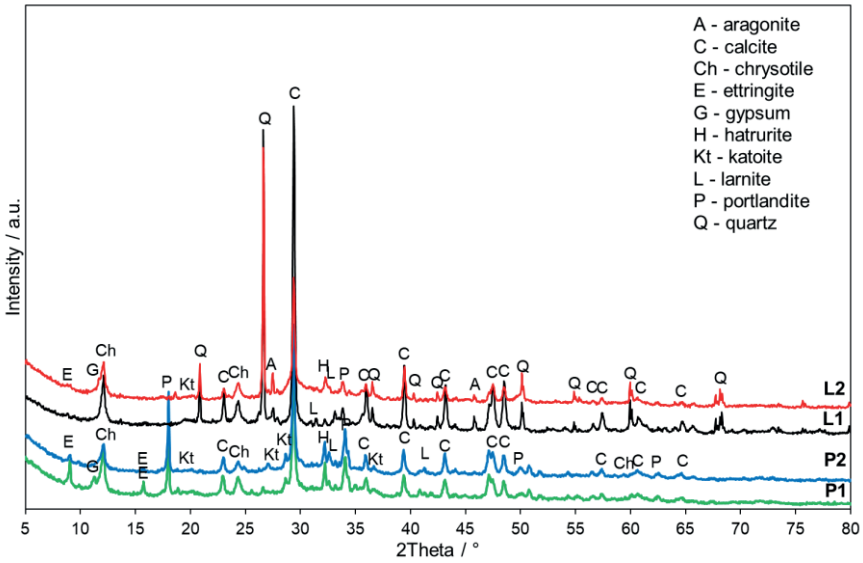

Fig. 2. XRD patterns of raw cement-asbestos materials from both countries.

For Lithuanian samples, mainly L2, x-ray reflexes associated with aragonite ($CaCO_3$; ICDD-PDF 01-085-6713) were also identified. Calcite-aragonite alternations and evolution are known and documented [36]. The formation of distinct $CaCO_3$ polymorphs can be explained by a combination of seasonal environmental changes (air temperature and water discharge). Aragonite is the high-temperature modification of anhydrous calcium carbonate minerals, but is well known to precipitate as an unstable phase in aqueous media near Earth's surface conditions. This phenomenon could have occurred during the long-term contact of Lithuanian samples with atmospheric moisture and rain.

The greatest differences in the phase composition of samples from both countries occur in the case of portlandite ($Ca(OH)_2$; ICDD-PDF 01-076-0571) and quartz (SiO_2; ICDD-PDF 01-086-1560). The first was identified only for Polish samples, while the second was confirmed only in samples coming from Baltic countries. The absence of calcium hydroxide in the cementitious matrix for samples coming from Lithuania confirmed the higher degree of ageing of these samples. As is well known, Portland cement during setting and ageing reacts with water, producing various hydrated compounds from which calcium silicate hydrates (the so-called CSH phase) and portlandite are the main [37], [38]. During long-term ageing and carbonation of the cementitious matrix, the calcium hydroxide converts into calcium carbonate in accordance with the reaction: $Ca(OH)_2 + CO_2 = CaCO_3 + H_2O$. In turn, Lithuanian samples have an evidently marked presence of quartz. This indicates probably a different production technology of cement–asbestos materials in the past in both countries or the original country from which the cement-asbestos materials were imported. In the case of Lithuanian samples, quartz sand was presumably used as a mineral filler for cement mass.

The thermal decomposition of all the examined cement-asbestos samples was qualitatively nearly identical. The effects resulting from the decomposition of the cementitious matrix dominated all obtained curves (Fig. 3). Between 100 °C and 200 °C, the endothermic peak can be connected with the mass change coming from the dehydration of CSH phase, i.e., calcium-silicate-hydrate phases, which are a group of compounds that are essential in the chemistry of cement and concrete. The CSH phase is a critical product formed during the

hydration of Portland cement and is responsible for most of the strength and durability of concrete [39], [40]. This effect is the strongest for the P1 sample which is connected also with the highest mass change (Fig. 4). In turn, for sample L1 this effect is weak and is associated with the small change of mass, which is visible for DTG curves (Fig. 5). This clearly indicates different ageing and weathering processes of the samples during long-term working in the outside environment what was also previously described. Moreover, for L2 and P2 samples, small inflexions of the DTG curves at ~200 °C can be observed. This effect can be associated with the thermal decomposition of gypsum, which decomposes into anhydrite with the release of water. The gypsum phase was found in the phase analysis of both samples (Fig. 2).

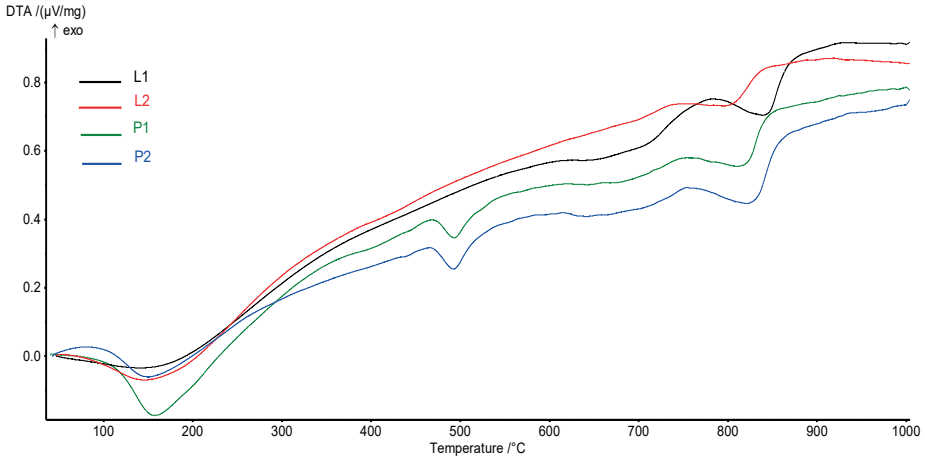

Fig. 3. DTA results for tested samples.

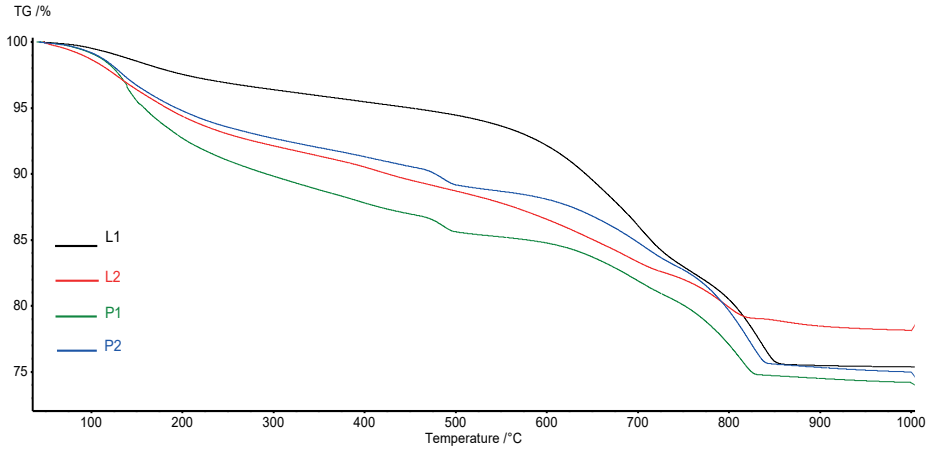

Fig. 4. TG results for tested samples.

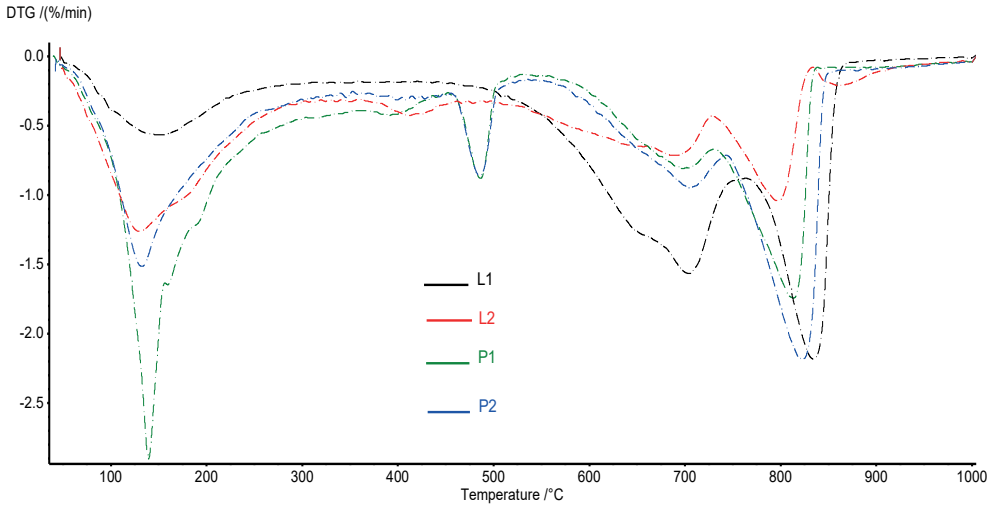

Fig. 5. DTG results for tested samples.

The endothermic peaks near 450 °C (clearly visible for P1 and P2 samples, Fig. 3) are associated with the thermal decomposition of portlandite. This effect is visible only in the case of Polish samples, especially as a small step on the TG curves and a well-marked effect on the DTG results. This observation is in line with the expectation from X-ray powder diffraction results (Fig. 2), where calcium hydroxide was identified only for P1 and P2 samples. At higher temperatures (in the range of 600–850 °C), two overlapping endothermic peaks were observed. They are more visible when we compare DTG results. The first one is weak, in a wide temperature range, and the second one has a characteristic asymmetric shape and a maximum at ~820 °C. The first effect occurs in the temperature range characteristic of the dehydroxylation process of chrysotile asbestos. Literature data show [18], [23], [35], [41] that this process for pure white asbestos is in the temperature range from 650 °C to 750 °C and is followed by solid-state recrystallisation at a temperature exceeding 800 °C into forsterite (Mg_2SiO_4) and enstatite ($MgSiO_3$) via the reaction: $Mg_3(OH)_4Si_2O_5 = Mg_2SiO_4 + MgSiO_3 + 2H_2O$. The second peak with an asymmetric shape and T_{max} above 800 °C is typical for the decomposition of calcium carbonate. It is worth noting that the maximum temperature of this effect is shifted to a higher temperature for the L1 sample, for which we expect the highest degree of carbonatisation, due to the highest value of loss on ignition (Table 1) as well as the strongest X-ray reflexes of calcite on the XRD pattern. Thermal decomposition of sulphur compounds was not detected due to the thermal analysis measurement conditions. They thermally decompose at the temperature range of 1200–1400 °C, especially calcium sulphate [42]–[48].

In turn, when we compare the chemical composition of cement–asbestos from both countries in the CaO-MgO-SiO_2 triangular diagram, some important differences can be reported (Fig. 6). Because the tested Lithuanian samples have quartz in their composition, the corresponding points in CaO-MgO-SiO_2 are lying closer to the point of pure silica. In contrast, Polish samples are located close to pure calcium oxide. According to the above-mentioned phase system, the change in the C/S ratio may influence the formation and synthesis of new compounds during thermal treatment. In the broadest context, the variable chemical compositions may affect the material's behaviour at high temperatures.

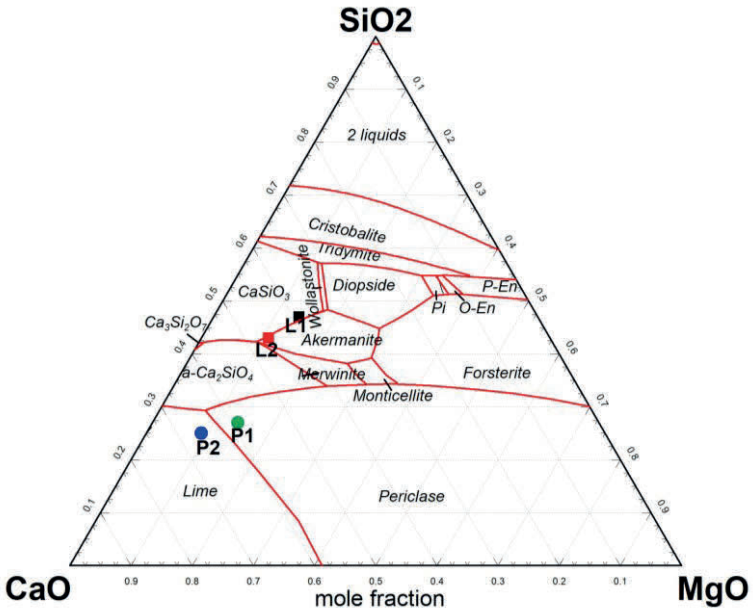

Fig. 6. Points corresponding to samples under study in the CaO-MgO-SiO_2 system.

As can be observed, Lithuanian asbestos wastes (marked as squares) constitute a separate group of wastes in terms of possible thermal treatment. Their chemical composition points distinctly lie in the area of increased SiO_2 content compared with that of Polish waste (points as circles) and simultaneously in other stability fields of phases in the equilibrium state. Moreover, when we consider CaO-MgO-SiO_2, there is a region of relatively low melting point minerals, centred on diopside $CaMgSi_2O_6$. If the CaO/SiO_2 ratio is <1.5, the liquids will form easily, especially at higher temperatures.

The above considerations were confirmed after analysing the samples after isothermal annealing. Fig. 7 presents the comparison of X-ray powder diffraction patterns of isothermally treated samples at 1100 °C for 2 h.

As we can see, from the mineralogical point of view materials obtained from both countries were varied. In the case of Polish samples, the main identified mineral phases were larnite (Ca_2SiO_4; ICDD-PDF 04-007-2687) as well as lime (CaO; ICDD-PDF 04-007-4743) and periclase (MgO; ICDD-PDF 01-087-0652). Moreover, for this type of sample, the phases like brownmillerite (Ca_2FeAlO_5, ICDD-PDF 04-011-5939), ye'elimite ($Ca_4(Al_6O_{12})SO_4$; ICDD-PDF 01-083-7086), and ternesite ($Ca_5(SiO_4)_2SO_4$; ICDD-PDF 04-009-4477) were identified. The presence of the main phases is in line with the considerations of the CaO-MgO-SiO_2 triangular diagram. Points of the chemical composition of these Polish samples are located near the triple point of stability fields of periclase, lime, and dicalcium silicate. The presence of phases containing sulphate anions results from the higher sulphur content in Polish waste (Table 1).

In turn, for the Lithuanian samples, their chemical composition points distinctly lie in the area of increased SiO_2 content compared with that of Polish waste and parallel in other stability fields of phases in the equilibrium state. Lithuanian samples crossed the stability fields of pseudo-wollastonite ($CaSiO_3$) and akermanite. As a result of isothermal treatment, the materials with the akermanite ($Ca_2MgSi_2O_7$; ICDD-PDF 04-014-4688), merwinite

($Ca_3MgSi_2O_8$; ICDD-PDF 00-035-0591), as well as bredigite ($Ca_{14}Mg_2(SiO_4)_8$; ICDD-PDF 00-036-0399) as main mineral phases were obtained (Fig. 7). Moreover, in both Lithuanian samples the presence of quartz (SiO_2; ICDD-PDF 01-086-1560) was also stated. Probably, this is silica from raw cement-asbestos samples, which don't react with the cementitious matrix under the considered conditions. For samples L1 and L2, the presence of clinoenstatite ($MgSiO_3$; ICDD-PDF 00-013-0415) and anorthoclase ($(Na,K)AlSi_3O_8$; ICDD-PDF 00-010-0361) was identified. The presence of phases not resulting from the ternary system under consideration is due to a more complicated chemical composition than that of the pure oxides. These other components also affect the synthesis of new phases.

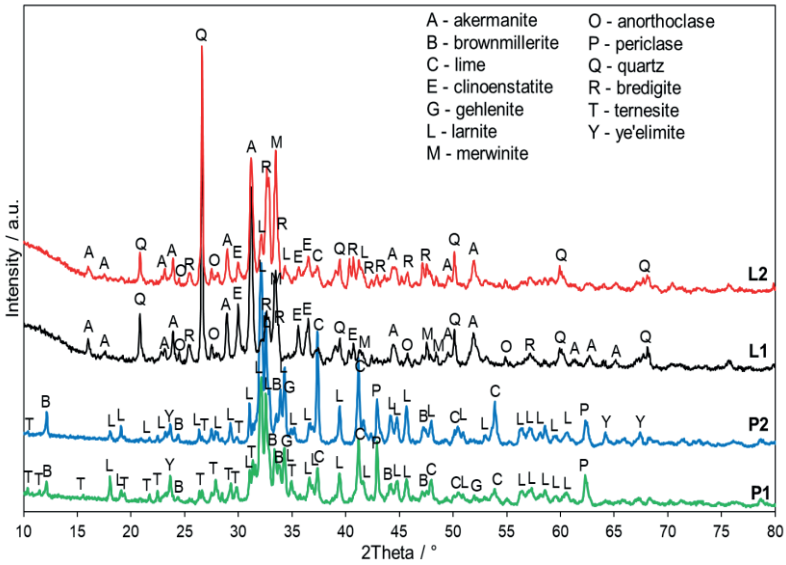

Fig. 7. XRD patterns of isothermally treated (1100 °C/2 h) cement-asbestos materials from both countries.

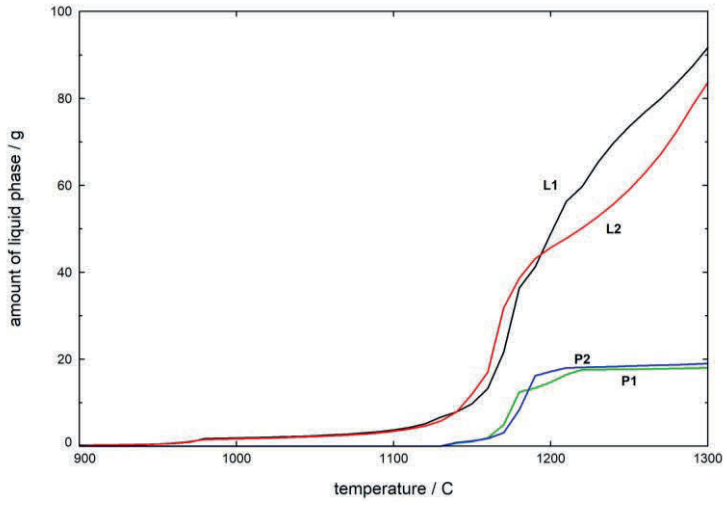

Fig. 8. Changes in the liquid phase amount during thermal treatment of the tested cement-asbestos samples.

In the broadest context, the variable chemical compositions may strongly affect the material's behaviour at high temperatures, especially for the creation of a liquid phase. From the engineering calculation (Fig. 8), the difference in the behaviour of the tested cement-asbestos samples is clearly and evidently visible. For Polish samples (P1 and P2), the first drops of the liquid phase should appear above 1150 °C. First, small amounts, to reach a level of about 20 % for temperatures above 1200 °C. Due to the similar chemical composition, both samples behave similarly. The chemical composition of samples from Lithuania reacts completely differently to the effect of temperature. As we can see in the graphic, the first drops of the liquid phase can appear at much lower temperatures, close to 1000 °C. At temperatures above 1100 °C, the amount of the liquid phase rapidly increases. At a temperature of 1200 °C, it constitutes about 50 wt% of the system and continues to grow with increasing temperature. For maximum calculation temperature, i.e., 1300 °C, we should get about 20 wt% of the liquid phase for Polish samples and over 90 wt% of this phase for Lithuanian cement-asbestos.

This behaviour was confirmed by tests in a high-temperature microscope. The obtained results (Table 2 and Table 3) show that at the temperature ~1000 °C materials begin to sinter and the liquid phase, especially for Lithuanian samples, was formed. With the increase in temperature, the sample softens. Changes in the cross-sectional area of the sample depend strongly on the source of the samples. Images recorded during the measurement for tested samples indicate that the amount of the liquid phase in the cement-asbestos sample increased significantly above 1250–1300 °C for Lithuanian samples, while for Polish samples it requires a temperature of about 100–150 °C higher.

TABLE 2. CHANGE OF CROSS-SECTION OF SELECTED SAMPLES DURING HIGH-TEMPERATURE MICROSCOPY ANALYSIS

Temperature; °C	**25**	**500**	**800**	**900**	**1000**	**1100**	**1200**	**1250**
L1	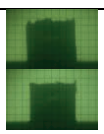	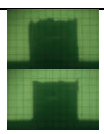	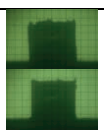	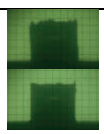	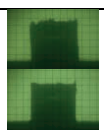	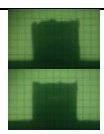	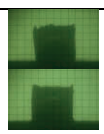	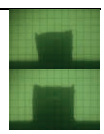
P1								
Temperature; °C	**1270**	**1280**	**1400**	**1420**	**1440**	**1450**	**1460**	**1470**
L1			-	-	-	-	-	-
P1						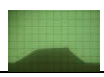		

TABLE 3. CHARACTERISTIC TEMPERATURES FROM HIGH-TEMPERATURE MICROSCOPY

Sample name	**sintering point; °C**	**softening point; °C**	**melting point; °C**	**flow point; °C**
L1	1050	1220	1230	1270
L2	980	1240	1320	1340
P1	1030	1250	1430	1450
P2	1040	1320	1420	1460

The difference found, and the clearly different behaviour of the tested cement-asbestos samples, encouraged us to undertake a literature review and calculate the amount of the liquid phase as well as the equilibrium composition for the other cement-asbestos samples described in the literature. In this context, for example, detailed information and data are provided by the work of Viani *et al*. [49], [50], who studied the crystal chemistry of raw as well as high-

temperature products of cement-asbestos samples from Italy. Based on the results of the authors, cement-asbestos samples revealed a complex mineralogy comprising up to 25 different phases. The authors divided the samples into three groups based on their dominant mineralogical composition: (i) samples lying on the boundary between the stability field of belite and periclase or well into the belite field, with high C/S ratio, (ii) samples falling prevalently into the stability field of merwinite, or (iii) samples whose corresponding points lay inside the stability field of akermanite, and diopside, with low C/S ratio.

Based on data found in the literature [14], [27], [49]–[70] (Annex; Table A1 and Fig. A1), the chemical composition of cement-asbestos samples may vary to some extent, especially in the context of the content of the main components, i.e., CaO and SiO_2. The calcium oxide content varies in a wide range from about 18 wt% to even above 60 wt%, while in the case of silicon oxide, it may change from about 15 wt% to 45–48 wt%. In turn, the amount of the third component, like magnesium oxide, may vary from ~2 wt% to about 10 wt%. All this influence on the composition points in the ternary CaO-MgO-SiO_2 system (Fig. A1). All cement-asbestos samples with an approximation lie along the curves defining the MgO composition at a level between 0.1 and 0.2 mole fraction, with a rather variable share of other ingredients. Moreover, we can observe that the tested Lithuanian samples were close to a group of samples indicated by Viani *et al*. [49], [50], whose corresponding composition points lay inside the stability field of akermanite. In turn, it can be found that Polish samples create an additional new group of cement–asbestos materials with high calcium oxide (CaO) content.

The thermochemical programme FactSage was used to obtain the liquid changes curve of the cement-asbestos materials from 900 °C to 1300 °C, as shown in Fig. A2. In the considered temperature range, cement-asbestos samples behave in a variety of ways, and it is difficult to provide an unambiguous classification in this respect. However, it can be seen that in the simulation course, the materials can be differentiated into several groups. The first group includes materials in which the visible amounts of liquid phase appear at a temperature between 950 °C and 1000 °C (including samples no. 1, 6, 27, 30, 41) and a further rapid increase of its amount. The second group includes materials in which the larger amount of liquid phase appears clearly at a temperature above 1100 °C (e.g., samples no. 4, 16, 27, 42). The considered Lithuanian samples (L1 and L2) fit into this group. The third group is samples for which the first droplets of the liquid phase are observed to appear above 1100 °C and up to the maximum simulation temperature; its increase is small (maximum up to approx. 20 wt%). Here could be classified the Polish samples P1 and P2. The next group includes materials with a low amount of the liquid phase remaining at a level of up to 5%, up to the maximum simulation temperature (samples no. 25, 28, 29). The last group includes materials in which the liquid phase did not appear in the entire range of the simulated heating temperature (for example, samples 34, 38, 44, 45, 46). Among all 60 materials, only one shows the appearance of the liquid phase at a temperature below 900 °C (sample no. 42), which results probably from the presence of the highest amount of potassium oxide (Table A1) in the composition.

These chemical differences may contribute to the formation of different mineral phases during thermal treatment, for example, in the context of the creation of liquid phase or mineral binder components. The equilibrium composition of cement-asbestos samples at 1100 °C, based on FactSage calculations, sorted by the amount of liquid phase, was presented in Fig. 9. As can be seen, for the considered samples, at least 15 different main mineral phases were identified that could appear in the material during isothermal treatment at the assumed temperature. Their quantity and quality strongly depend on the initial chemical composition of the material.

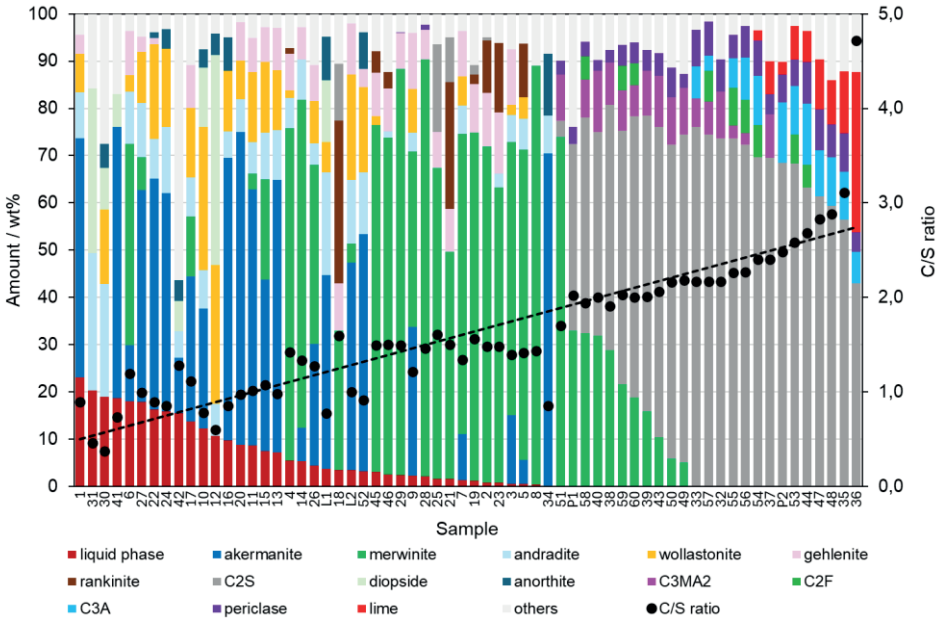

Fig. 9. Equilibrium composition of cement-asbestos samples at 1100 °C, based on FactSage calculations, sorted by the amount of liquid phase

There is a clear correlation between the appearance of the liquid phase and the change in the phase composition of the thermally processed material and its C/S ratio. The largest amounts of liquid phase should be formed for materials with low C to S coefficients, for samples with increased silica content. In this case, the main created mineral solid phase is akermanite. Next are samples for which the amount of liquid phase during thermal treatment is at a level of several per cent. In this case, merwinite or akermanite/merwinite phase will be created. When the C/S weight ratio achieves a value close to 2, in the system liquid phase isn't created, and C2S phase is dominated by mineralogical composition. In turn, for samples with the highest C/S ratio, additional free magnesium oxide as well as calcium oxide should also be expected in thermally treated samples.

4. DISCUSSION

The present study provides a comparative evaluation of cement-asbestos materials from Poland and Lithuania, focusing on their chemical composition, mineralogical phases, and thermal behaviour. The results demonstrate clear differences between cement–asbestos wastes originating from both countries. These differences could have important implications for waste management and potential thermal treatment routes; however, they must be interpreted with caution due to several limitations and sources of uncertainty.

The results highlight the influence of raw material selection and production methods on the thermal stability and transformation of these materials. Differences in the amounts of major oxides, strongly influence how the samples behave within the CaO–MgO–SiO_2 ternary system. The chemical analyses showed that Lithuanian samples contained higher SiO_2 and MgO contents, while Polish samples were richer in CaO and sulphur compounds. This composition influenced the thermal decomposition pathways, as evidenced by DTA/TG/DTG

analyses and high-temperature microscopy. The Lithuanian samples, for example, closely resemble the materials described by Viani *et al*. [49], [50] that fall within the akermanite stability field. This suggests that they share similar mineralogical and thermal characteristics. The Polish samples, on the other hand, form a distinct group with noticeably higher CaO content, which may affect how they respond to heating and which new mineral phases develop during thermal treatment. Lithuanian samples exhibited lower initial melting points and rapid formation of a liquid phase above 1100 °C, whereas Polish samples required higher temperatures (~1200 °C–1300 °C) for significant liquid phase formation. These differences are critical for designing thermal treatment processes and predicting the resulting mineral phases, which was also suggested by Italian researchers [49], [50].

XRD analysis confirmed that the primary asbestos mineral in all samples was chrysotile ($Mg_3Si_2O_5(OH)_4$), which decomposed into a new mineral phase upon heating above 800 °C. Due to the presence of the cementitious matrix, we do not observe the typical products of chrysotile asbestos degradation (such as forsterite or enstatite). Components of the cementitious matrix, such as portlandite and calcium carbonate, also underwent decomposition and contributed to the formation of new mineral phases, including larnite, akermanite, and merwinite. In the case of the latter two phases, Mg-rich compounds produced by asbestos decomposition were likely incorporated and combined with Ca-rich compounds, creating new phases characterised by low melting points. In contrast, under theoretical equilibrium conditions, the Polish samples favour the formation of free MgO in the reacted system.

The formation of new phases depends strongly on the CaO/SiO_2 (C/S) ratio [49], [50], which varied between samples from the two countries. Low C/S ratios favoured the formation of akermanite and liquid phases, while higher C/S ratios in the Polish samples resulted in stable crystalline phases with limited melting. Moreover, comparative analysis and thermodynamic calculations of the tested samples, as well as cement–asbestos materials described in the literature, clearly show that the Polish samples can be considered a separate group of cement–asbestos wastes, characterised by the highest C/S ratio. The strong contrast in liquid phase formation temperatures suggests that applying uniform thermal treatment protocols to all cement–asbestos waste may be ineffective or unsafe. Lithuanian samples, rich in SiO_2 and quartz, show a much earlier onset of melting, which could compromise process stability or energy efficiency. Polish samples, richer in CaO, maintain structural integrity to higher temperatures, favouring controlled sintering rather than extensive melting. Moreover, FactSage simulations assume equilibrium conditions and simplified oxide-based compositions. Real-world cement-asbestos contains additional minor elements and amorphous phases that may alter melting behaviour. Therefore, predicted liquid-phase quantities should be treated as indicative rather than exact.

The comparative analysis suggests that thermal treatment can effectively transform cement-asbestos materials, potentially enabling their reuse as secondary raw materials in construction applications. However, the variability in chemical composition indicates that treatment parameters must be adjusted according to the source material to optimise mineral phase formation and liquid yield. Limitations of the study include the small number of samples analysed and the lack of long-term field validation of the thermal treatment outcomes. Additionally, environmental factors, such as the ageing and weathering of the original materials, influenced their chemical and mineralogical properties. Future studies should expand the dataset to include a broader range of cement-asbestos materials and explore pilot-scale thermal treatment experiments to assess scalability and environmental safety. Despite these limitations, the combined experimental data and modelling consistently show that compositional differences between cement-asbestos wastes strongly influence their thermal

decomposition and melting behaviour. Lithuanian samples follow a low C/S compositional trend leading to early and extensive melting, while Polish samples behave like high-C/S materials forming Ca-rich phases. These differences should be considered when designing thermal detoxification or recycling processes.

5. CONCLUSIONS

Based on the research conducted, the following conclusions can be drawn: (1) Cement-asbestos materials from Poland and Lithuania exhibit significant differences in chemical composition and mineralogical structure, primarily related to CaO/SiO_2 ratios and magnesium content. These differences reflect distinct production methods and raw material sources; (2) Thermal decomposition of chrysotile asbestos and cementitious matrix components occurs in well-defined stages, resulting in the formation of secondary mineral phases such as periclase, larnite, akermanite, and merwinite; (3) Lithuanian samples, characterized by higher SiO_2 content, form liquid phases at lower temperatures (≈1000 °C–1100 °C), while Polish samples, richer in CaO, display higher thermal stability and liquid phase formation above 1150 °C; (4) The amount and type of mineral phases generated during thermal treatment are strongly dependent on the initial chemical composition, particularly the C/S ratio, which directly influences the potential for recycling these materials; (5) Thermal treatment offers a feasible route for neutralizing hazardous asbestos-containing waste and producing secondary raw materials suitable for construction applications, provided that treatment conditions are tailored to the chemical and mineralogical characteristics of the input material.

ACKNOWLEDGEMENT

This research was funded in whole by the National Science Centre, Poland, under "Sonata 17" grant number UMO-2021/43/D/ST5/00356.

ANNEX

TABLE A1. CHEMICAL COMPOSITION (WT%) OF CEMENT-ASBESTOS SAMPLES

Sample	SiO_2	TiO_2	Al_2O_3	Fe_2O_3	MnO	MgO	CaO	Na_2O	K_2O	P_2O_5	SO_3	L.O.I.	source
1	30.50	0.21	4.36	2.38	0.07	5.71	27.20	0.73	0.68	0.08	0.70	27.40	[49]
2	24.00	0.16	3.08	1.19	0.03	6.24	35.40	0.08	0.10	0.15	1.05	28.60	[49]
3	24.20	0.22	3.22	1.33	0.05	6.69	33.70	0.00	0.00	0.10	2.83	27.70	[49]
4	22.60	0.22	2.58	1.39	0.03	5.91	32.00	0.18	0.44	0.13	2.39	32.10	[49]
5	23.40	0.23	3.01	1.43	0.04	6.15	33.10	0.00	0.04	0.13	2.17	30.40	[49]
6	25.30	0.35	4.53	2.56	0.05	5.09	30.10	0.61	0.29	0.12	1.08	29.90	[49]
7	26.80	0.12	2.83	1.45	0.11	7.00	35.80	0.00	0.02	0.08	1.38	24.50	[49]
8	22.10	0.11	1.85	0.91	0.04	8.21	31.50	0.07	0.33	0.03	1.67	33.10	[49]
9	28.70	0.15	3.66	1.03	0.13	7.15	34.70	0.03	0.09	0.08	1.57	22.80	[49]
10	34.30	0.14	3.24	1.97	0.06	4.75	26.70	0.49	0.74	0.08	1.41	26.10	[49]
11	28.30	0.13	2.89	1.51	0.04	6.00	28.60	0.29	0.49	0.11	1.79	29.80	[49]
12	45.20	0.20	2.50	2.08	0.04	7.19	27.20	0.15	0.04	0.26	0.53	14.60	[49]
13	28.80	0.16	3.30	2.38	0.04	6.05	28.10	0.21	0.20	0.15	0.60	30.00	[49]
14	27.90	0.13	2.77	2.36	0.04	7.69	37.00	0.25	0.03	0.14	0.87	20.90	[49]
15	27.60	0.13	2.74	2.21	0.08	5.62	29.50	0.20	0.45	0.08	0.81	30.60	[49]
16	32.90	0.15	3.55	1.38	0.06	6.79	28.00	0.39	0.48	0.07	0.87	25.30	[49]

Sample	SiO_2	TiO_2	Al_2O_3	Fe_2O_3	MnO	MgO	CaO	Na_2O	K_2O	P_2O_5	SO_3	L.O.I.	source
17	26.20	0.19	4.06	1.95	0.07	4.55	29.20	0.46	1.04	0.10	4.16	28.00	[49]
18	21.80	0.13	2.70	1.26	0.15	2.45	34.60	0.11	0.36	0.11	3.18	33.10	[49]
19	21.90	0.14	2.80	1.71	0.08	6.38	34.10	0.02	0.04	0.10	3.27	30.40	[49]
20	29.20	0.15	3.20	1.61	0.04	7.01	28.30	0.27	0.23	0.08	0.50	29.50	[49]
21	25.60	0.13	2.60	1.45	0.07	4.38	38.40	0.18	0.14	0.10	1.12	25.90	[49]
22	31.50	0.15	3.06	1.99	0.04	5.39	28.10	0.52	0.54	0.09	0.58	28.00	[49]
23	24.80	0.15	3.66	1.59	0.09	5.74	36.80	0.00	0.01	0.05	1.96	25.10	[49]
24	31.50	0.14	3.41	3.23	0.09	5.13	26.70	0.58	0.49	0.08	0.28	28.50	[49]
25	22.70	0.12	2.14	1.21	0.04	5.70	36.50	0.02	0.06	0.04	1.94	29.50	[49]
26	25.70	0.15	2.63	1.08	0.04	6.27	32.70	0.15	0.34	0.03	4.41	26.40	[49]
27	28.30	0.14	2.93	2.62	0.04	5.48	27.90	0.61	0.60	0.17	1.65	29.60	[49]
28	22.10	0.12	1.90	0.64	0.04	7.86	32.30	0.01	0.11	0.04	0.59	34.40	[49]
29	23.60	0.14	2.40	0.88	0.04	7.72	35.20	0.03	0.03	0.07	1.27	28.70	[49]
30	48.73	0.20	3.67	6.27	0.19	1.47	18.10	0.25	0.46	0.08	n.a.	n.a.	[51]
31	43.74	0.23	2.16	14.87	1.31	6.13	19.97	n.a.	0.43	0.03	n.a.	n.a.	[51]
32	19.26	0.18	3.87	2.91	n.a.	5.78	41.80	0.03	0.36	n.a.	0.69	25.10	[52]
33	16.30	n.a.	3.43	n.a.	n.a.	5.12	35.40	n.a.	n.a.	n.a.	1.21	35.80	[53]
34	30.52	0.24	4.57	3.64	n.a.	7.70	25.83	0.60	0.27	n.a.	0.63	26.05	[54]
35	19.29	n.a.	3.81	3.98	n.a.	7.99	60.06	n.a.	n.a.	n.a.	2.99	n.a.	[55]
36	14.80	n.a.	2.47	4.44	n.a.	4.15	69.92	n.a.	0.27	n.a.	2.57	n.a.	[56]
37	19.72	n.a.	3.72	2.49	2.60	4.21	47.36	0.16	0.39	n.a.	0.69	18.05	[57]
38	21.60	n.a.	4.02	2.72	n.a.	5.34	41.30	0.21	0.29	n.a.	n.a.	n.a.	[58]
39	20.40	n.a.	3.85	2.89	n.a.	5.41	41.00	0.12	0.14	n.a.	n.a.	n.a.	[58]
40	21.30	0.23	5.09	2.29	0.15	5.94	42.50	0.16	0.25	n.a.	1.89	20.20	[59]
41	30.71	n.a.	2.19	8.32	0.02	10.19	22.36	2.16	0.07	n.a.	1.46	6.99	[70]
42	18.76	n.a.	4.75	1.46	0.50	2.63	23.98	0.57	1.62	n.a.	20.56	29.11	[60]
43	17.90	n.a.	4.40	2.30	n.a.	4.80	36.80	n.a.	0.75	n.a.	n.a.	20.20	[61]
44	18.20	n.a.	4.06	2.35	n.a.	7.27	48.69	n.a.	0.34	n.a.	1.66	16.30	[62]
45	21.86	0.16	2.55	n.a.	0.28	6.03	32.59	n.a.	0.27	0.21	2.61	27.86	[27]
46	21.51	0.16	2.57	3.94	0.29	6.12	32.28	n.a.	0.28	0.21	2.43	27.95	[27]
47	20.94	n.a.	3.59	3.43	n.a.	8.50	59.21	n.a.	n.a.	n.a.	2.11	n.a.	[63]
48	20.60	n.a.	3.88	4.79	n.a.	6.86	59.40	n.a.	0.65	n.a.	3.21	n.a.	[64]
49	19.74	0.18	3.72	3.01	0.04	3.48	43.02	0.16	0.15	0.11	2.20	23.98	[65]
50	19.11	0.15	3.77	3.30	0.08	5.94	41.30	0.21	0.13	0.09	1.35	24.12	[65]
51	21.45	0.14	3.63	2.72	0.06	9.89	36.51	0.05	0.01	0.06	1.38	23.81	[65]
52	32.10	0.20	3.90	3.10	0.00	5.60	29.20	0.10	0.30	0.00	0.60	24.70	[14]
53	17.80	n.a.	2.90	2.70	n.a.	4.30	45.90	n.a.	n.a.	n.a.	1.10	22.10	[66]
54	17.80	n.a.	2.90	2.90	n.a.	5.40	42.70	n.a.	n.a.	n.a.	1.50	23.30	[66]
55	18.50	n.a.	2.70	3.40	n.a.	3.70	41.90	n.a.	n.a.	n.a.	1.90	25.50	[66]
56	19.90	0.20	3.60	3.30	n.a.	5.40	45.20	0.10	0.30	n.a.	0.90	21.80	[67]
57	19.30	0.20	3.90	2.90	n.a.	5.80	41.80	0.10	0.40	n.a.	n.a.	25.10	[68]
58	20.67	n.a.	2.98	2.16	n.a.	5.85	40.02	n.a.	0.34	0.12	2.34	25.30	[69]
59	19.14	n.a.	3.02	2.20	n.a.	5.65	38.82	n.a.	0.31	0.11	2.53	25.90	[69]
60	20.30	n.a.	2.40	2.05	n.a.	5.36	40.54	n.a.	0.29	0.10	2.35	26.60	[69]
Average	***24.76***	***0.17***	***3.30***	***2.74***	***0.17***	***5.90***	***36.10***	***0.25***	***0.31***	***0.10***	***1.97***	***25.79***	

n.a. – not available; the value of 0 was assumed for calculations

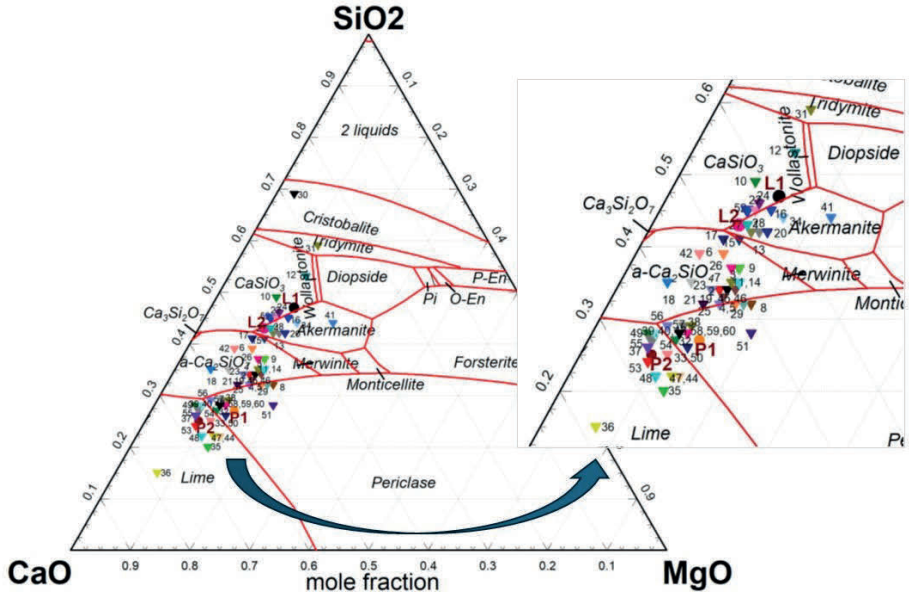

Fig. A1. Points corresponding to cement-asbestos samples under study and literature in the CaO-MgO-SiO_2 system.

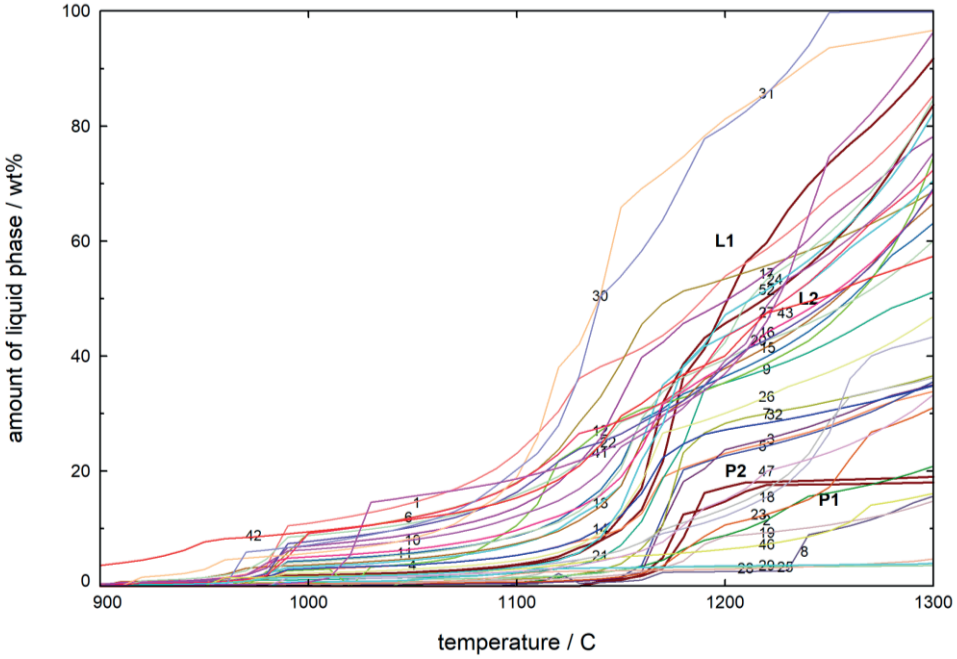

Fig. A2. Changes in the liquid phase amount during thermal treatment of considered cement-asbestos samples.

REFERENCES

[1] Carmignano O., Vieira, S., Brandão P. R., Bertoli A., Lago R. Serpentinites: Mineral Structure, Properties and Technological Applications. *Journal of the Brazilian Chemical Society* 2020:31:2–14. https://doi.org/10.21577/0103-5053.20190215

[2] Ciullo P. A., Industrial Minerals and Their Uses – a Handbook and Formulary, New York: William Andrew Publishing/Noyes, 1996. https://doi.org/10.1016/B978-081551408-4.50003-X

[3] Petrarca C., Viola D., Resta A., Di Giampaolo L., Wada H. Asbestos-Related and Non-Communicable Diseases in Formerly Exposed Workers: Relationship with Residential Asbestos, Smoke and Business Sector. *Journal of Community Medicine & Public Health* 2024:8:450. https://doi.org/10.29011/2577-2228.100450

[4] Takata A., Yamauchi H., Yamashita K., Aminaka M, Hitomi T., Toya T., Kohyama N. Mesothelioma Carcinogenesis of Chrysotile and Forsterite Compared and Validated by Intraperitoneal Injection in Rat. *Industrial Health* 2025:61(1):14–28. https://doi.org/10.2486/indhealth.2024-0025

[5] Harris L. V., Kahwa I. A. Asbestos: Old Foe in 21st-Century Developing Countries. *Science of the Total Environment* 2003:307:1–9. https://doi.org/10.1016/S0048-9697(02)00504-1

[6] LaDou J., Castleman B., Frank A., Gochfeld M., Greenberg M., Huff J., Joshi T. K., Landrigan P. J., Lemen R., Myers J., Soffritti M., Soskolne C. L., Takahashi K., Teitelbaum D., Terracini B., Watterson A. The Case for a Global Ban on Asbestos. *Environmental Health Perspectives* 2010:118/7:897–901. https://doi.org/10.1289/ehp.1002285

[7] Lin R.T., Chien L.C., Jimba M., Furuya S., Takahashi K. Implementation of National Policies for a Total Asbestos Ban: A Global Comparison. *Lancet Planet Health* 2019:3:341–348. https://doi.org/10.1016/S2542-5196(19)30109-3

[8] The International Ban Asbestos Secretariat IBAS [Online]. [Accessed 10.01.2025]. Available: www.ibasecretariat.org/index.htm

[9] Ulewicz M. Gospodarka materiałami azbestowymi w aspekcie bezpieczeństwa życia i pracy (Management of Asbestos Materials in Terms of Life and Work Safety). *Przegląd Budowlany* 2023:910:171–176. (in Polish) https://doi.org/10.5604/01.3001.0053.9394

[10] Flanagan D. M. Mineral Commodity Summaries. Asbestos 2022. Reston: Geological Survey, 2023.

[11] European Commission Directive 1999/77/EC, 26 July 1999; European Commission: Brussels, Belgium [Online]. [Accessed 10.01.2025]. Available: https://eur-lex.europa.eu/eli/dir/1999/77/oj

[12] Kusiorowski R., Lipowska B., Kujawa M., Gerle A. Problem of Asbestos-Containing Wastes in Poland. *Cleaner Waste System* 2023:4:1000085. https://doi.org/10.1016/j.clwas.2023.100085

[13] Smolianskiene G., Adamoniene D., Šeškauskas V. Studies on Occupational Asbestos in Lithuania: Achievements and Problems. *Indoor and Built Environment* 2005:14(3–4):331–335. https://doi.org/10.1177/1420326X05054294

[14] Kusiorowski R., Gerle A., Kujawa, M., Antonovič V., Boris R. Structural Characterisation of End-of-Life Cement-Asbestos Materials from Lithuania. *Fibers* 2024:12(4):37. https://doi.org/10.3390/fib12040037

[15] Paolini V., Tomassetti L., Segreto M., Borin D., Liotta F., Torre M., Petracchini F. Asbestos Treatment Technologies. *Journal of Materials Cycles and Waste Management* 2019:21:205–226. https://doi.org/10.3390/fib12040037

[16] Spasiano D., Pirozzi F. Treatments of Asbestos Containing Wastes. *Journal of Environmental Management* 2017:204(1):82–91. https://doi.org/10.1007/s10163-018-0793-7

[17] Iwaszko J. Making Asbestos-Cement Products Safe Using Heat Treatment. *Case Studies in Construction Materials* 2019:10:00221. https://doi.org/10.1016/j.cscm.2019.e00221

[18] Bloise A., Kusiorowski R., Lassinantti Gualtieri M., Gualtieri A F. Thermal Behaviour of Mineral Fibres. In Mineral Fibres: Crystal Chemistry, Chemical-Physical Properties, Biological Interaction and Toxicity. London: European Mineralogical Union, 2017:215–260. https://doi.org/10.1180/EMU-notes.18.7

[19] Bloise A., Catalano M., Barrese E., Gualtieri A.F., Gandolfi N.B., Capella S., Belluso E. TG/DSC Study of the Thermal Behavior of Hazardous Mineral Fibres. *Journal of Thermal Analysis and Calorimetry* 2016:123:2225–2239. https://doi.org/10.1007/s10973-015-4939-8

[20] Kusiorowski R., Gerle A., Kujawa M., Bloise A. Kinetic Aspects of Chrysotile Asbestos Thermal Decomposition Process. *Minerals* 2025:15:609. https://doi.org/10.3390/min15060609

[21] Bloise A. On the Thermal Breakdown of Tremolite: A New Method for Distinguishing Between Asbestos and Non-Asbestos Tremolite Samples. *Journal of Materials Science* 2023:58:8779–8795. https://doi.org/10.1007/s10853-023-08595-0

[22] Gualtieri A. F., Cavenati C., Zanatto I., Meloni M., Elmi G., Gualtieri M. L. The Transformation Sequence of Cement-Asbestos Slates up to 1200 °C and Safe Recycling of the Reaction Product in Stoneware Tile Mixtures. *Journal of Hazardous Materials* 2008:152:563–570. https://doi.org/10.1016/j.jhazmat.2007.07.037

[23] Cattaneo A., Gualtieri A. F., Artioli G. Kinetic Study of the Dehydroxylation of Chrysotile Asbestos with Temperature by in Situ XRPD. *Physics and Chemistry of Minerals* 2003:30:177–183. https://doi.org/10.1007/s00269-003-0298-2

[24] Gualtieri A. F., Levy D., Belluso E., Dapiaggi M. Kinetics of the Decomposition of Crocidolite Asbestos: A Preliminary Real-Time X-Ray Powder Diffraction Study. *Materials Science Forum* 2004:443-444:291–294. https://doi.org/10.4028/www.scientific.net/MSF.443-444.291

[25] Gualtieri A. F., Giacobbe C., Sardisco L., Saraceno M., Gualtieri M. L., Lusvardi G., Cavenati C., Zanatto I. Recycling of the Product of Thermal Inertization of Cement-Asbestos for Various Industrial Applications. *Waste Management* 2011:31:91–100. https://doi.org/10.1016/j.wasman.2010.07.006

[26] Gualtieri A. F., Tartaglia A. Thermal Decomposition of Asbestos and Recycling in Traditional Ceramics. *Journal of the European Ceramic Society* 2000:20(9):1409–1418. https://doi.org/10.1016/S0955-2219(99)00290-3

[27] Vergani F., Galimberti L., Marian N. M., Giorgetti G., Viti C., Capitani, G. Thermal Decomposition of Cement-Asbestos at 1100°C: How Much "Safe" is "Safe"? *Journal of Material Cycles and Waste Management* 2022:24:297–310. https://doi.org/10.1007/s10163-021-01320-6

[28] Bloise A. Thermal Behaviour of Actinolite Asbestos. *Journal of Materials Science* 2019:54:11784–11795. https://doi.org/10.1007/s10853-019-03738-8

[29] Giacobbe C., Gualtieri A.F., Quartieri S., Rinaudo C., Allegrina M., Andreozzi G.B. Spectroscopic Study of the Product of Thermal Transformation on Chrysotile-Asbestos Containing Materials. *European Journal of Mineralogy* 2010:22:535–546. https://doi.org/10.1127/0935-1221/2010/0022-2038

[30] Kim C., Kim Y., Roh Y. Thermal Decomposition and Phase Transformation of Chrysotile in Asbestos-Containing Waste. *Minerals* 2025:15:344. https://doi.org/10.3390/min15040344

[31] Curado A., Nunes L.J.R., Carvalho A., Abrantes J., Lima E., Tomé M. Recovery of End-of-Life Building Materials: Thermal Decomposition and Phase Transformation of Chrysotile in Asbestos-Containing Fiber Cement Boards. *Fibers* 2025:13:62. https://doi.org/10.3390/fib13050062

[32] Kusiorowski R., Gerle A., Kujawa M., Śliwa A. Influence of Thermally Treated Asbestos-Containing Materials on Cement Mortars Properties. *Applied Sciences* 2025:15:9225. https://doi.org/10.3390/app15169225

[33] Zhao-Hui H., Wen-Juan Li., Zi-He P., Yan-Gai L., Ming-Hao F. High-Temperature Transformation of Asbestos Tailings by Carbothermal Reduction. *Clays and Clay Minerals* 2013:61:75-82. https://doi.org/10.1346/CCMN.2013.0610106

[34] Worsztynowicz A., Mill W. Potential Ecological Risk Due to Acidification of Heavy Industrialized Areas – the Upper Silesia Case. *Studies in Environmental Science* 1995:64:353–365. https://doi.org/10.1016/S0166-1116(06)80296-7

[35] Zaremba T., Krzakała A., Piotrowski J., Garczorz D. Study on the Thermal Decomposition of Chrysotile Asbestos. *Journal of Thermal Analysis and Calorimetry* 2010:101:479–485. https://doi.org/10.1007/s10973-010-0819-4

[36] Eichiner S., Boch R., Baldermann A., Goetschl K., Wenighofer R., Hoffmann R., Stamm F., Hippler D., Grengg C, Immenhauser A., Dietzel M. Unravelling Calcite-to-Aragonite Evolution from a Subsurface Fluid – Formation Pathway, Interfacial Reactions and Nucleation Effects. *Chemical Geology* 2023:641:121768. https://doi.org/10.1016/j.chemgeo.2023.121768

[37] Dias C. M. R., Cincotto M. A., Savastano H., John V. M. Long-Term Aging of Fiber-Cement Corrugated Sheets - the Effect of Carbonation, Leaching and Acid Rain. *Cement and Concrete Composites* 2008:30(4):255–265. https://doi.org/10.1016/j.cemconcomp.2007.11.001

[38] Stepkowska E. T., Blanes J. M., Real C., Perez-Rodriguez J. L. Phase Transformation on Heating of an Aged Cement Paste. *Thermochimica Acta* 2004:420:79–87. https://doi.org/10.1016/j.tca.2003.11.057

[39] Hewlett P. C. Lea's Chemistry of Cement and Concrete. Arnold: J. Wiley, 1998.

[40] Taylor H. F. W. Cement Chemistry. London: Thomas Telford Publishing, 1997.

[41] Kusiorowski R., Zaremba T., Piotrowski J., Adamek J. Thermal Decomposition of Different Types of Asbestos. *Journal of Thermal Analysis and Calorimetry* 2012:109:693–704. https://doi.org/10.1007/s10973-012-2222-9

[42] Krejsová J., Kužel R., Keppert M., Scheinherrová L., Vimmrová A. New Insight into the Phase Changes of Gypsum. *Materials and Structures* 2024:57:128. https://doi.org/10.1617/s11527-024-02404-z

[43] Gerasimov M. V, Dikov Y. P, Yakovlev O. I, Wlotzka F. High-Temperature Vaporization of Gypsum and Anhydrite: Experimental Results. In: Abstracts of the 25th Lunar and Planetary Science Conference. Houston, USA,1994:45:413–414.

[44] Ingo G. M., Chiozzini G., Faccenda V., Bemporad E., Riccucci C. Thermal and Microchemical Characterizations of $CaSO_4$–SiO_2 Investment Materials for Casting Jewellery Alloys. *Thermochimica Acta* 1998:321:175–183. https://doi.org/10.1016/S0040-6031(98)00457-2

[45] Belardi C., Piga L. Influence of Calcium Carbonate on the Decomposition of Asbestos Contained in End-of-Life Products. *Thermochimica Acta* 2013:573:220–228. https://doi.org/10.1016/j.tca.2013.08.019

[46] Scrivener K., Nonat A. Hydration of Cementitious Materials, Present and Future. *Cement and Concrete Research* 2011:41(7):651–665. https://doi.org/10.1016/j.cemconres.2011.03.026

[47] Fukami T., Tahara S., Nakasone K., Yasuda C. Synthesis, Crystal Structure, and Thermal Properties of $CaSO_4 \cdot 2H_2O$ Single Crystals, *International Journal of Chemistry* 2015:7/2:12–20. https://doi.org/10.5539/ijc.v7n2p12

[48] Myka A. *et al.* Thermal Analysis of Materials Based on Calcium Sulphate Derived from Various Sources. *Journal of Thermal Analysis and Calorimetry* 2022:147:9923–9934. https://doi.org/10.1007/s10973-022-11319-2

[49] Viani A., Gualtieri A. F., Secco M., Peruzzo L., Artioli G., Cruciani, G. Crystal Chemistry of Cement-Asbestos. *American Mineralogist* 2013:98:1095–1105. https://doi.org/10.2138/am.2013.4347

[50] Viani A., Gualtieri A. F., Pollastri S., Rinaudo C., Croce A., Urso G. Crystal Chemistry of the High Temperature Product of Transformation of Cement-Asbestos. *Journal of Hazardous Materials* 2013:248–249:69–80. https://doi.org/10.1016/j.jhazmat.2012.12.030

[51] Dellisanti F., Minguzzi V., Morandi N. Experimental Results from Thermal Treatment of Asbestos Containing Materials. *GeoActa* 2001:1:61–69.

[52] Witek J., Mróz H., Barański J., Brach J. Neutralisation of Asbestos-Containing Waste Using the Method of Melting in an Arc Resistance Furnace. *Prace Instytutu Ceramiki i Materiałów Budowlanych* 2012:5/11:146–58 (in Polish).

[53] Radvanec M., Tuček L., Derco J., Čechovská K., Németh Z. Change of Carcinogenic Chrysotile Fibers in the Asbestos Cement (Eternit) to Harmless Waste by Artificial Carbonatization: Petrological and Technological Results. *Journal of Hazardous Materials* 2013:252–253:390–400. https://doi.org/10.1016/j.jhazmat.2013.02.036

[54] Giacobbe C., Gualtieri A. F., Quartieri S., Rinaudo C., Allegrina M., Andreozzi G. B. Spectroscopic Study of the Product of Thermal Transformation of Chrysotile- Asbestos Containing Materials (ACM). *European Journal of Mineralogy* 2010:22(4):535–546. https://doi.org/10.1127/0935-1221/2010/0022-2038

[55] Iwaszko J., Zawada A., Przerada I., Lubas M. Structural and Microstructural Aspects of Asbestos-Cement Waste Vitrification. *Spectrochimica Acta Part A: Molecular and Biomolecular Spectroscopy* 2018:195:95–102. https://doi.org/10.1016/j.saa.2018.01.053

[56] Iwaszko J., Lubas M., Sitarz M., Zajemska M., Nowak A. Production of Vitrified Material from Hazardous Asbestos-Cement Waste and CRT Glass Cullet. *Journal of Cleaner Production* 2021:317:128345:1–12. https://doi.org/10.1016/j.jclepro.2021.128345

[57] Staněk T., Boháč M., Zezulová A., Rybová A. Hydraulic Binder from Hazardous Waste. *Solid State Phenomena* 2018:276(2):3–8. https://doi.org/10.4028/www.scientific.net/SSP.276.3

[58] Pawełczyk A., Bożek F., Grabas K., Chęcmanowski J. Chemical Elimination of the Harmful Properties of Asbestos from Military Facilities. *Waste Management* 2017:61:377–385. https://doi.org/10.1016/j.wasman.2016.11.041

[59] Lázár M., Hnatko M., Sedláček J., Čarnogurská M., Brestovič T. Upgrading the Glassy Slag from Waste Disposal by Thermal Plasma Treatment. *Waste Management* 2018:78:173–182. https://doi.org/10.1016/j.wasman.2018.05.042

[60] Colangelo F., Cioffi R., Lavorgna M., Verdolotti L., De Stefano L. Treatment and Recycling of Asbestos-Cement Containing Waste. *Journal of Hazardous Materials* 2011:195:391–397. https://doi.org/10.1016/j.jhazmat.2011.08.057

[61] Znamenáčková I., Dolinská S., Lovás M., Hredzák S., Matik M., Tomčová J., Čablík V. Application of Microwave Energy at Treatment of Asbestos Cement (Eternit). *Earth and Environmental Science* 2016:44:(5):052023. https://doi.org/10.1088/1755-1315/44/5/052023

[62] Santana H. A., Amorim Júnior N. S., Carneiro G. O., Ribeiro D. V., Cilla M. S., Dias C. M. R. Asbestos-Cement Wastes as Supplementary Precursors of NaOH-Activated Binders. *Construction and Building Materials* 2023:364:129921. https://doi.org/10.1016/j.conbuildmat.2022.129921

[63] Iwaszko J., Making Asbestos-Cement Products Safe Using Heat Treatment, *Case Studies in Construction Materials* 2019:10:e00221. https://doi.org/10.1016/j.cscm.2019.e00221

[64] Lim Y., Jang H., So S. Evaluation of Mineral Carbonation of Asbestos-Tex and Analysis of Airborne Asbestos Concentrations. *Buildings* 2022:12/9:1372. https://doi.org/10.3390/buildings12091372

[65] Kusiorowski R., Gerle A., Kujawa M., Śliwa A., Adamek J. Characterisation of Asbestos-Containing Wastes by Thermal Analysis. *Journal of Thermal Analysis and Calorim*etry 2024:149:10681–10694. https://doi.org/10.1007/s10973-024-13312-3

[66] Kusiorowski R. Study on the Thermal Decomposition Process and Disposal of Cement-Asbestos Materials. Doctoral dissertation, Silesian University of Technology, 2014.

[67] Witek J., Kusiorowski R. Neutralization of Cement-Asbestos Waste by Melting in an Arc-Resistance Furnace. *Waste Management* 2017:69:336–345. https://doi.org/10.1016/j.wasman.2017.08.017

[68] Witek J., Psiuk B., Naziemiec Z., Kusiorowski R. Obtaining an Artificial Aggregate from Cement-Asbestos Waste by the Melting Technique in an Arc-Resistance Furnace. *Fibers* 2019:7/2:10. https://doi.org/10.3390/fib7020010

[69] Stevulova N., Estokova A., Holub M., Singovszka E., Csach K. Characterization of Demolition Construction Waste Containing Asbestos, and the Release of Fibrous Dust Particles. *Applied Sciences* 2020:10/11:4048. https://doi.org/10.3390/app10114048

[70] Dellisanti F., Rossi P.L., Valdrè G. Remediation of Asbestos Containing Materials by Joule Heating Vitrification Performed in a re-pilot Apparatus. *International Journal of Mineral Processing* 2009:91:61–67. https://doi.org/10.1016/j.minpro.2008.12.001